

# SIMULATION OF FLOOD CONTROL BY RAINWATER STORAGE FACILITIES IN URBANIZED WATERSHED

Agus SUHARYANTO<sup>1</sup>, Satoru SUGIO<sup>2</sup>, Chikashi DEGUCHI<sup>3</sup> and Masato KUNITAKE<sup>4</sup>

<sup>1</sup>Member of JSCE, Ph.D., Junior Lecturer of Civil Eng., Brawijaya University/Former Graduate student of United Graduate School Kagoshima University (Jalan Mayjen Haryono 167, Malang 65145, Indonesia)

<sup>2</sup>Member of JSCE, Dr. of Eng., Professor, Dept. of Civil and Environmental Eng., Miyazaki University (Gakuen Kibanadai-nishi 1-1, Miyazaki 889-21, Japan)

<sup>3</sup>Member of JSCE, Dr. of Eng., Assoc. Professor, Dept. of Civil and Environmental Eng., Miyazaki University (Gakuen Kibanadai-nishi 1-1, Miyazaki 889-21, Japan)

<sup>4</sup>Member of JSCE, Dr. of Agr., Professor, Dept. of Agriculture Eng. and Forest Science, Miyazaki University (Gakuen Kibanadai-nishi 1-1, Miyazaki 889-21, Japan)

The percentage of impervious area is estimated from satellite remote sensing data and is used to simulate runoff discharge in an urbanized watershed. To control the water level during flooding, the rainwater storage facilities by means of house storage and public storage are examined. From the simulated results it can be seen that the rate of increase in the peak water level reduces according to the increase of percentage of impervious area and that the rainwater storage facilities are effective for decreasing the occurrence of inundation by lowering the water level, however, are not so effective to lower the water level in the inundated area.

*Key Words* : percentage of impervious area, urbanized watershed, analysis of infiltration, rainfall excess, flood routing, peak water level, house storage, public storage

## 1. INTRODUCTION

Increasing the impervious area in urbanized watershed has direct effect to the increasing of runoff discharge and to the occurrence of inundation<sup>1</sup>. The changes of impervious area are related to the changes in landcover conditions in the watershed. To improve the increasing of runoff discharge and thereby to prevent the occurrence of inundation, it is necessary to apply the flood control in the watershed. There are many methods of flood control in the urbanized watershed<sup>2</sup>. Among them, infiltration facilities and storage facilities are already in operation in many cities in Japan. The flood control by means of infiltration facilities has been deeply discussed by Nagasawa and Minagawa<sup>3</sup>.

On the flood control by means of storage facilities, the detention basin has been examined by the runoff discharge simulation with Nash method<sup>4</sup>. The rainwater storage facilities by house storage and public storage may also be promising to the mitigation of inundation damage in urbanized watershed. To evaluate the effect of the rainwater storage facilities, however, it is necessary to evaluate

the change in landcover conditions and to develop the runoff discharge model. Changes in landcover conditions can be estimated from satellite remote sensing data<sup>5,6</sup>. Satellite remote sensing data have some advantages over aerial photographs or ground surveys. Satellite remote sensing is capable of wide areas observation, possible to obtain multispectral scanning and time series data. From the multispectral scanning data a kind of landcover can be discriminated by computer processing.

The aims of this paper are (1) to evaluate the effectiveness of house storage installed in impervious area and public storage installed in pervious area to control water level in the flood, (2) to develop the runoff discharge model which can evaluate the changes of percentage of impervious area in urbanized watershed, and (3) to examine the usefulness of the percentage of impervious area estimated from satellite remote sensing data as one of the input data for the runoff discharge model.

The effectiveness of the rainwater storage facilities is evaluated by comparing the water levels simulated without facilities with those simulated by application of facilities at the same station.

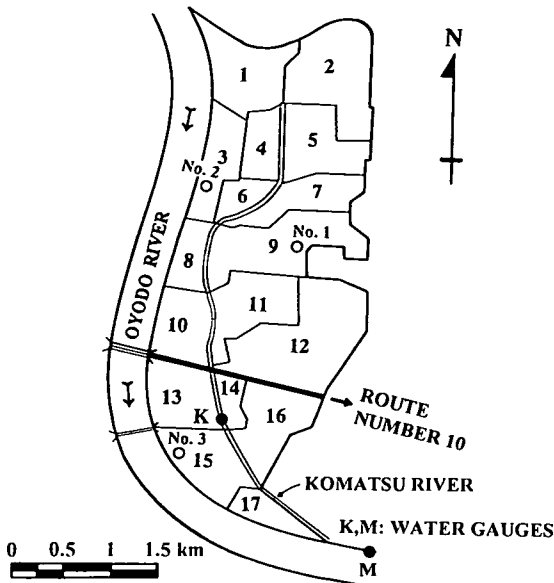


Fig.1 Outline of Komatsu watershed.

## 2. RESEARCH WATERSHED

The study area is Komatsu watershed, which occupies 3.5 km<sup>2</sup> of commercial-residential land. This watershed is located in the central part of Miyazaki city, Kyushu island, Japan. In this watershed, Komatsu river which is 3.5 km long flows through the city and is a tributary of Ohyodo river. Komatsu river only has a water level gauge K at about 1050 m from its outlet. By considering the drainage conditions, the Komatsu watershed is divided into 17 subbasins. Fig.1 shows the outline of Komatsu watershed.

This watershed is chosen for research because of the following reasons; the urbanization in the upstream part seems to be notable and the watershed has been damaged by the inundation in several times, although the discharge is very small on fine days. Drainage system is not completely furnished yet, and greater runoff volume is drained to the river by overland flow.

## 3. FUNDAMENTAL EQUATIONS

A numerical runoff discharge model was constructed to simulate the water level in the flood in Komatsu watershed<sup>7)</sup>. The numerical model consists of three submodels. The first submodel is an unsaturated seepage model to evaluate the rainfall excess intensity from the observed rainfall. This submodel termed rainfall excess model is developed

to adapt the rainwater storage facilities. The second and third submodels are the flood routing models to calculate the overland flow in the subbasin (termed surface runoff model) and unsteady flow in the river (termed flood routing model), respectively. The runoff discharge model is applied to simulate the effect of flood control by means of rainwater storage facilities.

### (1) Rainfall excess model

There are many methods to compute the rainfall excess, such as Horton infiltration method, the  $\phi$  index method, etc.<sup>8)</sup> In this research, the rainfall excess is evaluated theoretically by an analysis of infiltration into the surface soil under the assumption that a great part of rainfall loss during rainstorms in urbanized watershed is caused by infiltration into the ground surface. The physical process of infiltration is analyzed by the numerical simulation of unsaturated seepage flow into the surface soil<sup>9),10)</sup>.

To identify the unsaturated seepage parameters of the surface soil, three measuring points (No.1 ~ No.3) shown in Fig.1 are selected from the public spaces for the field measurements<sup>11)</sup>. After the observation, the infiltration flow is numerically simulated by Finite Elements Method using unsaturated characteristic curves estimated by Van Genuchten equation expressed as follows<sup>12)</sup>.

$$Se = 1 / \left\{ 1 + (a|\psi|^b) \right\}^m$$

$$kr = Se^{1/2} \left[ 1 - (1 - Se^{1/m})^m \right]^2 \quad (1)$$

$$kr = \frac{ku}{ks}, \quad Se = \frac{\theta - \theta_r}{\theta_s - \theta_r}, \quad m = 1 - \frac{1}{b}$$

where,  $\psi$  is capillary suction (cm),  $\theta$  is volumetric water content (cm<sup>3</sup>/cm<sup>3</sup>),  $\theta_r$  is residual water content,  $\theta_s$  is saturated water content,  $a, b, m$  are Van Genuchten coefficients,  $ku$  and  $ks$  are unsaturated and saturated hydraulic conductivity (m/s), respectively.

The rainfall excess is evaluated by the numerical analysis of the vertical one dimensional unsaturated seepage flow<sup>13)</sup>. The governing equation is expressed as shown in Eq.(2).

$$\frac{\partial \theta}{\partial t} = - \frac{\partial i}{\partial z}, \quad i = -ku \frac{\partial \psi}{\partial z} + ku \quad (2)$$

boundary conditions :  $i_1 = r : \theta_1 < \theta_s$

$$i_1 = r : \theta_1 = \theta_s \wedge r < i_2$$

$$i_1 = i_2 : \theta_1 = \theta_s \wedge r \geq i_2$$

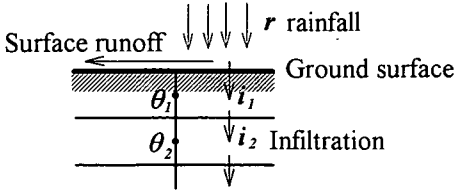


Fig.2 Surface runoff generation

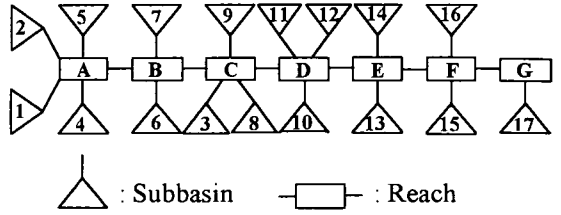


Fig.3 Outline of Komatsu watershed flow diagram

where  $i$  is infiltration rate (m/s), the subscripts are the numbers of discretized cell from the ground surface, and  $r$  is rainfall intensity (m/s). As shown in the boundary conditions, after the calculated volumetric water content at the topmost cell  $\theta_1$  reaches  $\theta_s$  and if the rainfall intensity exceeds  $i_2$ , only a part of rainfall infiltrates into the ground of pervious surface and the other part flows down on the surface as shown in Fig.2. Besides this, on the impervious surface, no rainfall infiltrates into the ground.

Assuming house storage only stores the rainwater in impervious areas and public storage catches it in pervious areas, the rainfall excess can be calculated by the following equations.

$$\begin{aligned}
 r_E &= \alpha r D (1 - \beta) + \alpha r D \beta \delta & : r < i_1 \\
 r_E &= \alpha r D (1 - \beta) + \alpha r D \beta \delta & : r \geq i_1 \text{ \& } \\
 &+ (\alpha r - i_1) ((1 - D) - A_P / A_S) & S_P \leq V_P \\
 r_E &= \alpha r D (1 - \beta) + \alpha r D \beta \delta & : r \geq i_1 \text{ \& } \\
 &+ (\alpha r - i_1) (1 - D) & S_P \geq V_P
 \end{aligned}
 \tag{3}$$

$$\begin{aligned}
 \delta &= 0 : S_H < V_H, \quad \delta = 1 : S_H \geq V_H \\
 S_H &= \sum A_H r \Delta t, \quad V_P = A_P h_P \\
 S_P &= \sum (\alpha r - i_1) A_P \Delta t
 \end{aligned}$$

where,  $r_E$  is rainfall excess (m/s),  $D$  is percentage of impervious area, which is defined as the ratio of impervious area to subbasin area,  $\alpha$  is coefficient related to rainfall loss except infiltration, for example, evaporation, depression storage, etc.<sup>14)</sup>,  $\beta$  is ratio of total catching area for house storage facility to total impervious area,  $\delta$  is parameter decided by house storage volume  $V_H$  and stored rainwater volume in the house storage  $S_H$  ( $m^3$ ),  $A_H$  is caching area ( $m^2$ ) for house storage facility,  $A_P$  is area for public storage facility ( $m^2$ ),  $h_P$  is public storage depth (m),  $A_S$  is total area of subbasin ( $m^2$ ),  $V_P$  is public storage volume ( $m^3$ ) and  $S_P$  is stored rainwater volume in public storage ( $m^3$ ). There is normal surface runoff from every subbasin when the public storage and house storage is completely full or  $\beta=0$ ,  $A_P=0$ .

## (2) Surface runoff model

The rainfall excess of the every subbasin flows down into the river as overland flow of each subbasin. The whole watershed is simplified and modeled in a net which is composed by a set of rectangular subbasins and a set of reaches. Fig.3 shows the outline of this net. The overland flow is simulated by kinematic waves method. The governing equations of this flow are expressed as follows<sup>15)</sup>:

$$h = \left( N / \sqrt{S} \right)^{0.6} q^{0.6}, \quad \frac{\partial h}{\partial t} + \frac{\partial q}{\partial x} = r_E \tag{4}$$

where,  $h$  is depth of overland flow (m),  $S$  is slope of subbasin,  $q$  is discharge per unit width ( $m^3/s/m$ ) and  $N$  is effective roughness coefficient of Manning's formula, which is related with the urbanization rate in the following equation<sup>16)</sup>:

$$N = 1.3 \times 10^{-2.1U} \tag{5}$$

where,  $U$  is urbanization rate, which is defined as the ratio of artificial area (except agricultural land) in the watershed to the whole watershed area. In this definition, fully artificialized area contains some pervious area. Assuming a simple linear equation between urbanization rate and percentage of impervious area, the next equation is applied instead of Eq.(5) in this submodel.

$$N = C_1 \times 10^{-C_2 D} \tag{6}$$

The discharge at the downstream end of subbasin corresponds to the inflow rate in the flood routing analysis.

## (3) Flood routing model

The dynamic waves method is applied for the flood routing analysis of the river. In this submodel the movement of a flood wave through a river is simulated by the method of characteristics using the governing equation expressed as follows<sup>17)</sup>:

Table 1 Parameters of infiltration characteristics

Points	No.1	No.2	No.3
Soil	Silt loam	Silt loam	Sandy loam
$\theta_r$	0.30	0.30	0.0001
$\theta_s$	0.4442	0.3925	0.3531
$a$	0.0878	0.0915	0.0760
$b$	6.203	5.598	5.696
$ks$	1.7E-6 m/s	1.7E-6 m/s	1.7E-6 m/s

$$\frac{\partial v}{\partial t} + v \frac{\partial v}{\partial x} + g \frac{\partial h}{\partial x} = g \left( S_0 - \frac{n^2 v^2}{R^{4/3}} \right) \quad (7)$$

$$\frac{\partial A}{\partial t} + \frac{\partial Q}{\partial x} = q_j \quad (8)$$

where,  $v$  is velocity of flow (m/s),  $h$  is depth of flow (m),  $R$  is hydraulic radius (m),  $S_0$  is slope of reach,  $n$  is Manning's roughness coefficient,  $A$  is cross sectional flow area (m<sup>2</sup>),  $Q$  is discharge (m<sup>3</sup>/s) and  $q_j$  is inflow rate from subbasin per unit width (m<sup>3</sup>/s/m).

The boundary condition at the downstream end of the river is given as the water level observed at water gauge M in the Ohoyo river shown in Fig.1. The boundary condition at the upstream end is given as both the total discharge of subbasins No.1 and No.2 and the water depth assumed to be normal depth determined from the discharge because the both values are required by the code of the method of characteristics used in this research.

#### 4. PARAMETER ESTIMATION

##### (1) Rainfall excess model

The unsaturated seepage parameters at three measuring points No.1~No.3 are identified from the field measurements. By assuming homogeneity of the surface soil and approximating  $\theta_s$  value as the measured porosity, the unknown parameters in Eq. (1) are  $a, b, \theta_r$  and  $ks$ . These unknown parameters are modified to make the calculated infiltration rates agree with the measured results. Finally the approximated parameters are obtained as shown in Table 1 and the characteristic curves are shown in Fig.4. Comparing these curves, the Komatsu watershed is assumed to be classified geohydrologically into two regions, which are divided by route No.10 shown in Fig.1. The characteristics curve on the northern side of route No.10 is assumed to be the averaged curve of points No.1 and No.2, and on the southern side is assumed to be equal to that of point No.3.

After unsaturated characteristic curves of surface soil are identified, the rainfall excess calculation can

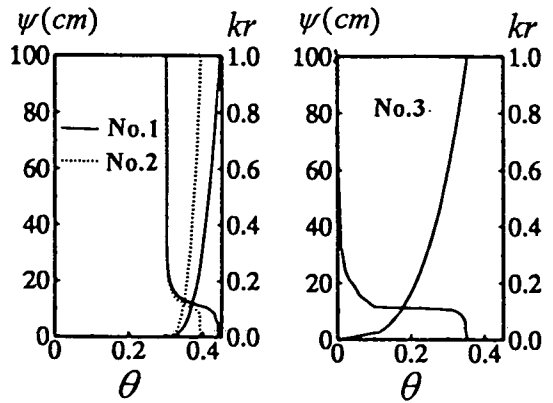


Fig.4 Unsaturated characteristic curves

Table 2 Representative subbasin dimensions

No.	Area(m <sup>2</sup> )	Slope	No.	Area(m <sup>2</sup> )	Slope
1	288,793	0.015	10	196,747	0.010
2	359,471	0.006	11	234,907	0.004
3	174,983	0.010	12	438,578	0.010
4	117,729	0.011	13	201,065	0.006
5	198,289	0.011	14	76,716	0.010
6	92,131	0.007	15	207,307	0.004
7	158,323	0.010	16	222,144	0.004
8	108,159	0.007	17	77,995	0.008
9	340,661	0.007			

be done. The infiltration rate is simulated by Eq.(2) with assumption that the groundwater table is 1.9 m deep. The initial water content in the unsaturated zone is assumed to be distributing linearly from the measured value at the ground surface to the saturated value at the groundwater table. The values of  $dz$  and  $dt$  are decided as 1 cm and 60 sec., respectively, and the calculated infiltration rates are checked with the rainfall intensity for all time steps.

##### (2) Surface runoff model

The overland flow is simulated by Eq.(4) together with Eq.(6). The dimensions of subbasins shown in Table 2 are obtained from the surveyed results. The other parameter is effective roughness coefficient of Manning's formula  $N$ . It is very difficult to estimate the  $N$  parameter in the urbanized watershed such as the Komatsu watershed, because the landcover is very complex.

To estimate the parameters  $C_1, C_2$  in Eq.(6) and parameter  $\alpha$  in Eq.(3), the runoff discharge model is applied to simulate the water level response on Sept. 25, 1983 under the normal surface runoff conditions with  $\beta=0$  and  $A_p=0$ . To make the simulated result agree with unique response of observed water level in the rising limb of flood, only these parameters ( $\alpha, C_1,$

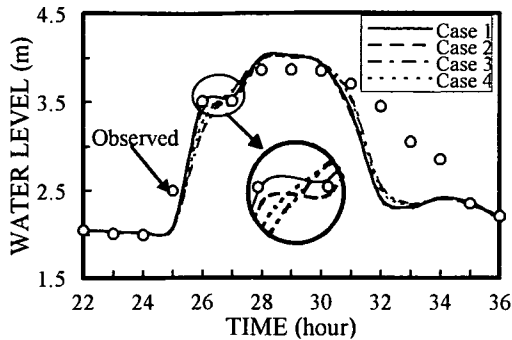


Fig.5 Water level changes according to the changes of  $\alpha$ ,  $C_1$  and  $C_2$  in the rainstorm of 25/9/83

$C_2$ ) are changed. Some of these simulated results are shown in Fig.5. In this Figure, case 1 is  $\alpha=0.85$ ,  $C_1=1.1$ ,  $C_2=2.4$ ; case 2 is  $\alpha=0.80$ ,  $C_1=1.1$ ,  $C_2=2.4$ ; case 3 is  $\alpha=0.85$ ,  $C_1=2.0$ ,  $C_2=2.4$  and case 4 is  $\alpha=0.85$ ,  $C_1=1.1$ ,  $C_2=2.0$ . Finally suitable values are selected to be  $\alpha=0.85$ ,  $C_1=1.1$  and  $C_2=2.4$ .

### (3) Flood routing model

The Komatsu river is a tributary of Ohyo river. When the water level of Ohyo river is higher than Komatsu river, the Komatsu river sluice gate which is located at the outlet will be closed. To satisfy the boundary conditions at the downstream end described above, the flood routing model has a restriction condition; i.e. this model can only be used in the opened condition of the sluice gate. This condition is controlled by comparison of the water levels observed at water gauges M and K. The cross-sectional shape of Komatsu river is assumed to be rectangular in this analysis. Komatsu river has no levee and faces the roads on both sides and also some parts of the ground surface in the right side of river are lower than the left side parts enough to be inundated in the rainstorm. Fig.6 shows the conceptual vertical cross-section used in the analysis for these parts. When the calculated water depth  $h$  exceeds the channel depth  $z^*$ , the water is considered to inundate the ground surface on the right side of river. Consequently the value of water depth is assumed to be reduced by spreading in the 50 m wide section to have equal cross-sectional area. The dimensions of Komatsu river as shown in Table 3 are decided from surveyed results. The Manning's roughness coefficient is estimated to be 0.03 from observed mean velocity in a flood. By using Eq.(7) and Eq.(8) with  $dx=50$  m and  $dt=5$  sec., the flood routing is simulated.

To evaluate the simulated results, the simulated and observed water levels of Komatsu river are compared at water level gauge K.

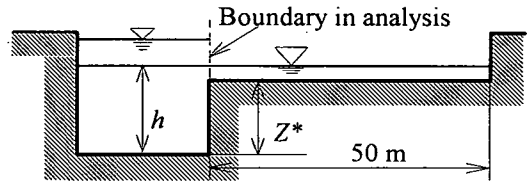


Fig.6 Conceptual cross-section of Komatsu river

Table 3 Representative channel dimensions

Distance (m)	Bed elev.(m)	Depth (m)	Width (m)
3500	5.01	2.00	4.20
3150	4.39	2.00	5.00
2700	3.67	2.81	5.00
2450	2.62	2.36	7.10
2100	2.47	2.25	7.60
1750	2.13	2.61	7.60
1400	1.85	2.13	7.50
1050	1.69	2.80	7.50
700	1.06	2.86	7.50
350	0.52	3.73	7.50
0	-0.26	5.00	8.10

## 5. PERCENTAGE OF IMPERVIOUS AREA

Estimation of percentage of impervious area from satellite remote sensing data needs landcover classified from satellite image. The classification was done by combining Ward Clustering algorithms and Nearest Neighbor classification methods<sup>18)</sup>. Nine landcover categories are usually classified. Among them, High Density, Medium Density and Low Density categories are considered to contribute to the impervious area of the watershed. The percentage of impervious area can be estimated by multiplying each pixel number of High Density, Medium Density and Low Density by Modification Coefficients and then divide by whole number of pixels of every subbasin. The Modification Coefficients are conversion parameters of High Density, Medium Density and Low Density with values from 5% to 100%.

Table 4 shows the satellite remote sensing and the aerial photograph data used in this research. By comparison between the percentage of impervious area interpreted from aerial photograph in 1987 and those estimated from SPOT-HRV and LANDSAT-TM data observed in 1988, the Modification Coefficients are decided<sup>19)</sup>. The values are 75%, 65% and 50% for High Density, Medium Density and Low Density categories, respectively. By using these Modification Coefficients, the percentages of impervious area after 1988 are estimated from satellite data<sup>20)</sup>. To check the estimated results using

Table 4 Aerial photograph and satellite remote sensing data

Data	Sensor	Date	Ground resolution
SPOT	HRV	20.12.1988	20 × 20m
		06.06.1990	
		09.01.1991	
LANDSAT	TM	20.12.1988	30 × 30 m
		22.07.1991	
		05.03.1993	
Aerial Photo.		1962, 1966	1:10000, 1:10000
		1971, 1983	1:23000, 1:22000
		1987, 1991	1:13000, 1:12500

Table 5 Percentage of impervious area of watershed

Sub-basin	Aerial Photograph			H R V			TM
	'83	'87	'91	'88	'90	'91	'93
1	44.1	55.5	55.7	43.2	48.0	56.9	51.5
2	51.0	52.0	53.0	43.4	46.6	55.9	56.4
3	34.8	43.9	50.4	38.3	36.5	53.5	54.6
4	53.2	56.2	62.7	63.0	68.3	69.7	66.7
5	40.6	34.3	52.6	43.0	52.2	57.3	63.2
6	52.8	55.6	67.6	60.1	62.8	66.6	67.9
7	45.5	54.1	51.0	48.6	52.7	50.9	64.7
8	32.7	36.0	47.3	31.1	38.4	45.3	45.9
9	47.0	47.4	50.0	44.6	49.9	57.0	62.4
10	44.8	49.8	69.9	57.6	58.1	66.6	65.9
11	53.2	58.6	63.5	59.1	66.8	66.0	65.4
12	57.2	62.1	67.8	63.1	68.9	70.5	66.4
13	53.6	63.1	73.5	63.5	66.1	69.1	66.5
14	61.1	64.8	69.6	65.7	69.0	69.2	72.5
15	54.7	60.3	65.6	65.5	65.8	65.8	67.9
16	69.1	70.9	74.9	65.4	69.2	69.0	69.5
17	64.7	65.0	72.6	64.4	66.9	66.4	66.4
Mean	48.5	52.9	61.6	53.3	55.7	62.1	63.0

the selected Modification Coefficients, the percentage of impervious area in 1991 is interpreted. Table 5 shows the interpreted and estimated results from 1983 to 1993. It can be seen that the interpreted and estimated results in 1991 agree well.

## 6. SIMULATION OF WATER LEVEL IN THE FLOOD

To test the validity of the proposed runoff discharge model to evaluate the change of landcover condition, the model is applied to simulate the water level in the flood by using the decided parameters and the observed rainfall intensity. The rainfall data are selected when the water levels at water gauge K are high enough to those in Ohoyo river observed at water gauge M. The public storage facility in Culture park, located in subbasins No.2 and No.5 as shown in Table 6, has been in operation since 1991. Consequently, the observed water levels from 1991

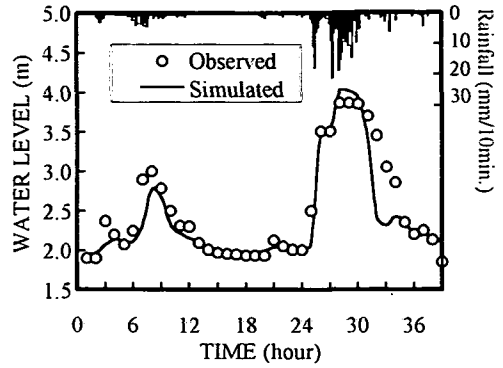


Fig.7 Water level response on 25/9/83

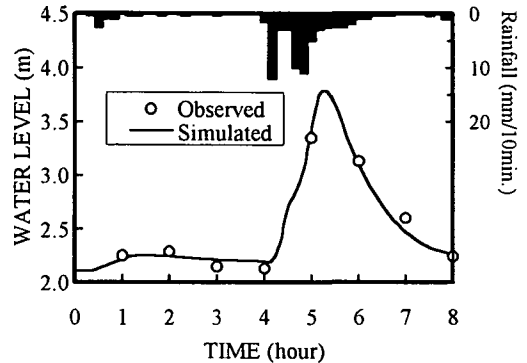


Fig.8 Water level response on 7/5/90

are affected by this public storage. The house storage facility is not installed in this area. The parameters in Eq.(3), therefore, are selected as  $\beta=0$  and  $A_p=0$  in Fig.7 ~ Fig.8 and  $\beta=0$  in Fig.9. The percentages of impervious area used in the simulations are interpreted from aerial photographs (before 1988) and estimated from satellite remote sensing data (from 1988). The water levels of simulated results are compared with the water levels of observed results at water level gauge K. Fig.7 ~ Fig.9 show the comparison of water levels during rainstorm. From these figures it can be seen that the simulated water levels agree well with the observed water levels. The inundation was observed in the rainstorm shown in Fig.7. The inundation location, where the water depth is higher than channel height, can be seen from the longitudinal water profile at the peak time at water gauge K shown in Fig.10. Assuming the water surface on the ground which has the same elevation in orthogonal direction to the river with it in the river, the inundation areas are estimated by finding the areas where the ground level is less than assumed water level. Fig.11 shows the comparison of inundated areas. The estimated result agrees with

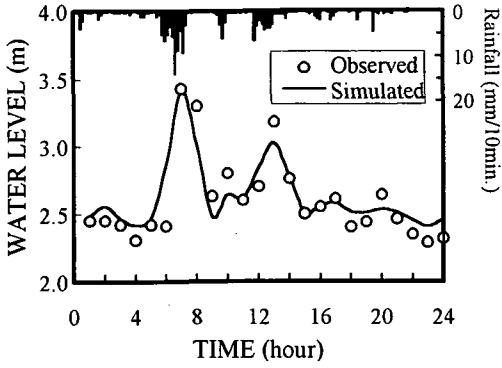


Fig.9 Water level response on 26/7/'93

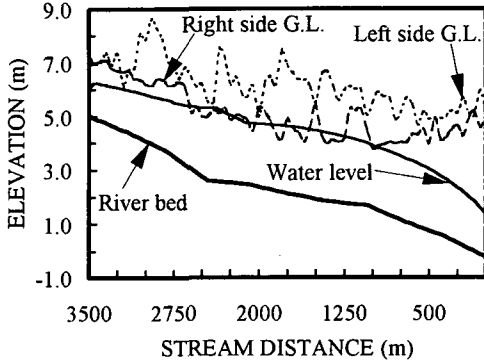


Fig.10 Longitudinal water profile on 25/9/'83

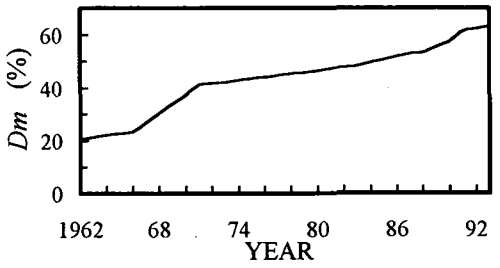


Fig.12 Change of mean percentage of impervious area

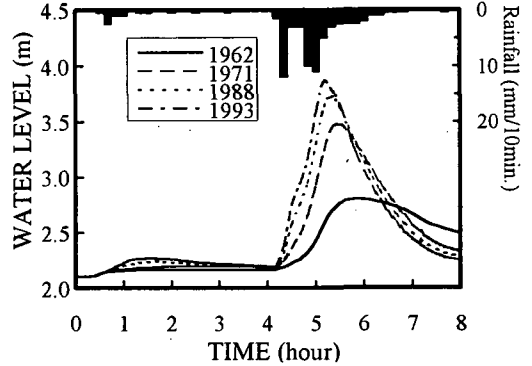


Fig.13 Water response to 7/5/'90 rainstorm

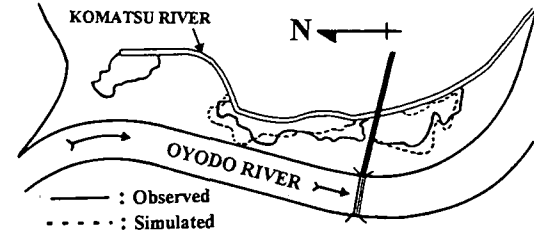


Fig.11 Comparison of inundated areas

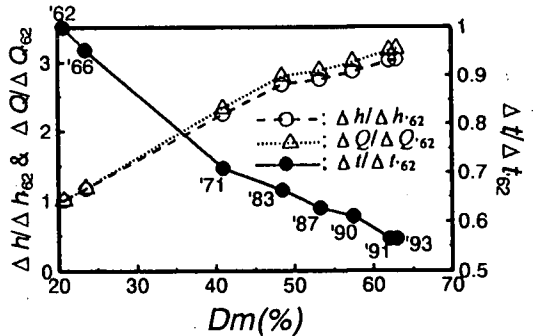


Fig.14 Relation between  $\Delta h$ ,  $\Delta Q$ ,  $\Delta t$  and  $D_m$

observed one except around the upstream end. In the upstream end, it is considered that inundation may be caused by the poor outflow in the process of overland flow as usual in the heavy rainstorm. From these results the validity of the proposed runoff discharge model can be confirmed.

The runoff discharge model is applied to estimate the change of flood according to the increase of percentage of impervious area. The rainstorm data observed on May 7, 1990 is used to the simulations. Fig.12 shows the change of mean percentage of impervious area in the whole subbasin ( $D_m$ ) from 1962 to 1993. Fig.13 shows the change of water level at water gauge K according to the change of

percentage of impervious area from 1962 to 1993. From this result it can be seen that the changes of water levels are conspicuous as the past result<sup>8)</sup>. The peak water levels from year to year are higher and faster according to the increase of percentage of impervious area. Fig.14 shows the changes of  $\Delta h$  (difference of water levels in rising limb),  $\Delta Q$  (difference of discharges in rising limb) and  $\Delta t$  (elapsed times in rising limb) at water level gauge K. It can be seen that the relation between  $\Delta h$ ,  $\Delta Q$  and  $D_m$  is nonlinear and the rates of increase in  $\Delta h/\Delta h_{62}$  and  $\Delta Q/\Delta Q_{62}$  are reducing in high percentage of impervious area. This is caused by the fact that the increase of percentage of impervious area in the

upstream part is bigger than it in the downstream part in the last decade as shown in Table 5, and then the effect of far subbasin to the flow at water gauge K is less than it of near subbasin.

## 7. ASSESSMENT OF FLOOD CONTROL

The runoff discharge model is applied to simulate the flood control by means of rainwater storage facilities, especially house storage and public storage. To know the effect of flood control in the present landcover condition, the latest percentage of impervious area in 1993 is used in the simulation.

### (1) House storage facility

The house storage facility is considered to function like water storage tank to catch rainwater from the roof and the paved parking lot in each house. In this research, the catching area for one storage tank is assumed to be 30% of roof area per house. The roof area of each house measured in Komatsu watershed was distributed randomly. From the measured result, the mean roof area per house is equal to 138.0 m<sup>2</sup>.

To evaluate the effectiveness of installed house storage in each subbasin to lower the peak water level at water gauge K, the preliminary case, that the discharge from the individual subbasin is completely stopped, is simulated on July 26, 1993 rainstorm. From the simulated results it is found that subbasins No.5, No.9, No.10 and No.13 have relatively big effect to the water level at water gauge K. Therefore in the following simulations, the house storage facilities are assumed to be concentrically installed only in these subbasins.

The peak water level at water gauge K on July 26, 1993 rainstorm (total rainfall 159 mm) is simulated in several combinations of  $V_H$  and  $\beta$  under the condition of  $A_P=0$ . Fig.15 shows the water level changes at water gauge K according to the changes of  $V_H$  and  $\beta$ . It can be seen that the effective volume of house storage is equal to 3 m<sup>3</sup> to lower the water level at water gauge K, because of that decreasing peak water level is the same when the installed  $V_H$  exceeds 3 m<sup>3</sup> for each  $\beta$  value. This case can be understood that the stored rainwater volume until the peak time (6.5 hours) is equal to 2.82 m<sup>3</sup>. It means that the rainwater from catching area until 6.5 hours can fill the house storage facility of  $V_H=3$  m<sup>3</sup> in this case. Increasing  $V_H$  more than 3 m<sup>3</sup> has the effect to lower the water level after the peak time, but the storage volume become too big for the house storage facility.

By the same method the runoff discharge model is

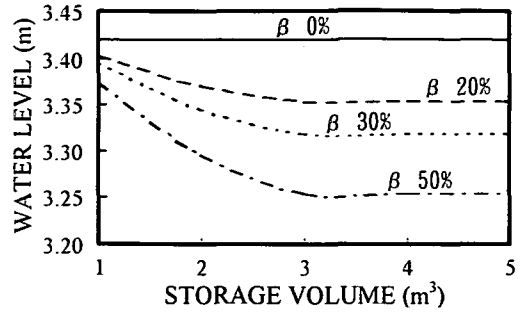


Fig.15 Decrease of peak water level on 26/7/'93 rainstorm

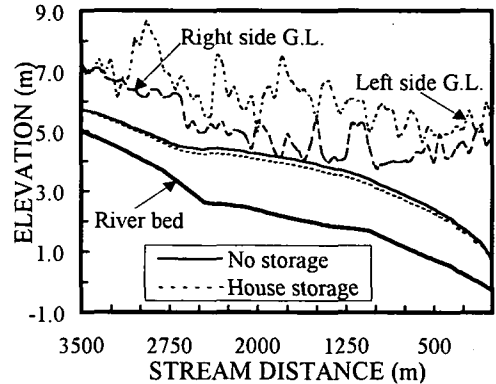


Fig.16 Longitudinal water profile at the peak time of the 26/7/'93 rainstorm

applied to simulate the changes in water level for the Sept. 25, 1983 (total rainfall 407 mm and 190 mm in 3 hours in the peak time) and May 7, 1990 (total rainfall 70 mm) rainstorms. From the simulated results the effective volume of house storage for May 7, 1990 rainstorm is equal to 2 m<sup>3</sup>. However, in the case of Sept. 25, 1983 rainstorm, the stored rainwater volume until the peak time (28 hours) is equal to 13 m<sup>3</sup>. Hence, a minimum of 13 m<sup>3</sup> house storage volume is necessary to decrease the peak water level in this case. But actually it is very difficult to installed the house storage facility with very big volume like this.

Fig.16 shows the longitudinal water profile of peak water level before (no storage) and after installation of the house storage facility ( $V_H=3$  m<sup>3</sup> and  $\beta=50\%$ ). Fig.17 and Fig.18 show the water level responses in Sept. 25, 1983 and May 7, 1990 rainstorms after installation of  $V_H=3$  m<sup>3</sup> and  $\beta=50\%$ . It can be seen that the water level in the flood is lowered by the installation of house storage, but the peak water level at 28 hours in Fig.17 is practically not lowered by the installation of house storage because of quite



Table 6 Dimensions and locations of public storage

Area	Sub-basin No.	$A_S(m^2)$	$h_P(m)$	$A_P(m^2)$
Culture park	2	366530	1	70200
	5	192687	1	89550
Demizuguchi park	3	174983	1	30778
Public University	7	183470	0.2	37540
	9	346221	0.2	32500
Miyazaki Shogyo Senior high school	10	196747	1	42350
Huzoku El. School	12	438578	1	34375
Nishiike El. School	12	438578	1	23444
Odo El. School	15	207307	0.2	16397

smaller storage volume than the rainwater volume to be stored.

From these results it can be concluded that the house storage facility is effective to decrease the occurrence of inundation by lowering the water level in the flood, however, is not effective to lower the peak water level in this research.

(2) Public storage facility

The second type of rainwater storage facility is public storage facility. In this research public storage facility means the rainwater is stored on the ground in pervious areas such as public parks and school athletic fields. In case of Komatsu watershed, there are 6 more suitable public spaces for new public storage facility except Culture park. Table 6 shows the dimensions and locations as public storages. The runoff discharge model is applied to simulate the changes of water level after installation of all public storage without house storage. Fig.17 and Fig.18 also show the water level response after installation. In Fig.17, the inundation occurs at 28 hours. Although the water level before occurrence of inundation is lowered by the installation, the smaller effect of the installation is simulated during the inundation. The difference of water level response is considered to be caused by the fact that the change of water level is shortened and becomes dull by spreading the water surface in the inundated areas. From these results, it can be seen that the public storage facility has effect similar to the house storage facility to lower the water level in the floods, but also it is not so effective to lower the inundated water level such as in the peak time during the Sept. 25, 1983 rainstorm.

Fig.17 and Fig.18 also show the water level responses after installation of the combination of house storage ( $V_H = 3 m^3$ ,  $\beta = 50\%$ ) and all of public storage facilities. It can be seen that the combination has big effect to lower the water level on May 7, 1990 rainstorm, but still small effect on Sept. 25,

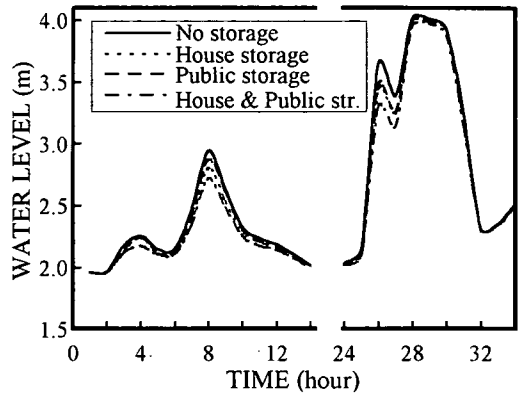


Fig.17 Effect of storage facilities during the 25/9/'83 rainstorm

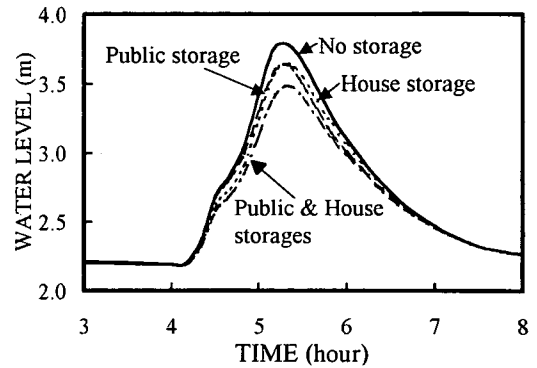


Fig.18 Effect of storage facilities during the 7/5/'90 rainstorm

1983 rainstorm.

From these results, it is clear that the water level before occurrence of inundation is lowered according to the installation of rainwater storage facilities. However, effect of the installation is not evident to lower the inundated water level. Therefore, it can be concluded that the rainwater storage facilities can decrease the occurrence of inundation by lowering the water level in the flood.

8. CONCLUSIONS

The simulations and results of this paper can be summarized as follows:

1. From the agreement between the simulated and observed water levels, the validity of the numerical runoff discharge model to evaluate the change of landcover conditions can be confirmed.
2. From the agreement between the simulated and observed water levels, it can be recommended that the percentage of impervious area estimated from satellite remote sensing data can be used as

an input data to express the change of runoff discharge according to the urbanization in watershed.

3. The rate of increase in the peak water level reduces according to the increase of mean percentage of impervious area in whole subbasin.
4. The rainwater storage facilities by means of house storage facility in the impervious area, public storage facility in the pervious area and the combination of these facilities are effective to decrease the occurrence of inundation by lowering the water level in the flood.
5. The effective volume of house storage to lower the peak water level is dependent on the total rainfall up to the peak time.

**ACKNOWLEDGMENT:** The authors would like to thank Foundation of River and Basin Integrated Communications, Japan, for their financial support and Miyazaki Work Office of Ministry Construction for supporting this research.

#### REFERENCES

- 1) Kadoya, M.: A Review of The Study on Runoff Changes Due to Urbanization, *Proc. of JSCE*, No. 363/II-4, pp. 23-34, 1985.
- 2) Musiaki, K.: Hydrological System in Urban Areas, *Jour. of Society of Hydrology & Water Resources*, Vol.2, No.1, pp.23-32, 1989.
- 3) Nagasawa, Y. and Minagawa, K.: The Storm Water Infiltration System in Housing and Urban Development Corporation, *Usuigijyutsushiryō, Assoc. for Rainwater Storage and Infiltration Technology*, Vol.1, pp. 65-98, 1991.
- 4) Kitagawa, Y., Sukegawa, N. and Nonaka, M.: Simulation of The Effect of Runoff Control of Stormwater Detention Facilities by a Flood Runoff Model, *Jour. of Hydraulic, Coastal and Envir. Eng., JSCE*, No.497/II-28, pp.21-29, 1994.
- 5) Engman, E.T. and Gurney, R.J.: *Remote Sensing in Hydrology*, Chapman and Hall, pp. 85-99, 103-125, 1991.
- 6) Ragan, R.M. and Jackson, T.J.: Runoff Synthesis Using Landsat and SCS Model, *Jour. of The Hydraulics Division, ASCE*, Hy5, pp. 667-677, May 1980.
- 7) Sugio, S. and Deguchi, C.: Simulation of Stormwater Discharge from Small Urban Watershed, *Proc. of Sixth Int. Conference on Urban Storm Drainage*, IAHR/IAWQ, Canada, pp. 579-584, 1993.
- 8) Bedient, P.B. and Huber, W.C.: *Hydrology and Floodplain Analysis*, 2nd ed., Addison-Wesley Publishing Co., New York, pp. 87-148, 239-309, 1990.
- 9) Neumen, S.P.: Saturated-Unsaturated Seepage by Finite Elements, *Proc. ASCE*, Hy12, Vol. 99, pp. 2233-2250, 1973.
- 10) Akai, K., Onishi, Y. and Nishigaki, M.: Finite Element Analysis of Saturated-Unsaturated Seepage in Soil, *Proc. of JSCE*, No. 264, pp.87-96, 1977.
- 11) Sugio, S. and Okabayashi, T.: Unsaturated Permeability of Shirasu and Its In-Situ Measuring Methods, *Jour. of Hydraulic, Coastal and Envir. Eng., JSCE*, No. 503/II-29, pp. 39/47, Nov. 1994.
- 12) Zaradny, H.: *Groundwater Flow in Saturated and Unsaturated Soil*, A.A. Balkema, Rotterdam, pp. 19-81, 1993.
- 13) Oka, T., Kadoya, M. and Noguchi, Y.: Rainfall Infiltration and Runoff Characteristics in an Urban Area, *Annuals, Disaster Prevention Research Institute, Kyoto Univ.*, No. 23B, pp. 227-238, 1980.
- 14) Chadwick, A. and Morfett, J.: *Hydraulics in Civil and Environmental Engineering*, E & FN SPON, London, pp. 327-335, 1993.
- 15) Kawamura, S.: *Hydrology and Hydraulics 1*, Morikita, Tokyo, pp. 85-98, 1984.
- 16) Musiaki, K., Ishizaki, K., Yoshino, F. and Yamaguchi, T.: *Conservation and Renewal of Water Environment*, Sankaido, Tokyo, pp. 54-74, 1987.
- 17) Kawamura, S., Fujita, I. and Nakatani, T.: *Hydraulic Exercise with Personal Computer*, Morikita, Tokyo, 1985.
- 18) Mather, P.M.: *Computer Processing of Remotely-Sensed Images An Introduction*, Biddles Ltd. Chichester, pp. 125-152, 276-329, 1987.
- 19) Deguchi, C. and Sugio, S.: Estimations for Percentage of Impervious Area by The Use of Satellite Remote Sensing Imagery, *Wat. Sci. Tech.* Vol. 29, No. 1-2, pp. 135-144, 1994.
- 20) Suharyanto, A., Deguchi, C., Sugio, S. and Kunitake, M.: Use of Satellite Data in Monitoring Impervious Area in Urbanized Area, *Proc. of LASTED International Conference*, Gold Coast, Australia, pp. 159-164, 1996.

(Received August 19, 1996)

## 都市河川流域における雨水貯留施設による洪水制御の予測シミュレーション

アグス スハリャント・杉尾 哲・出口 近士・國武 昌人

不浸透面積率を衛星リモートセンシングデータから推定し、この値を都市河川流域の流出解析に適用した。これにより、洪水時の水位に対する各戸雨水貯留施設および公共雨水貯留施設の制御効果を検討した。この解析結果から、洪水ピーク水位の増加率は流域全体の不浸透面積率の増大にともなって減少すること、また、雨水貯留施設は、洪水時の水位の低下によって浸水の発生を減少させる効果を持つが、浸水後の水深の低下にはそれほど効果がないことなどが明らかになった。